

Osteoarthritis and Cartilage

Increased susceptibility to develop spontaneous and post-traumatic osteoarthritis in *Dot1l*-deficient mice

F.M.F. Cornelis †, A. de Roover †, L. Storms †, A. Hens †, R.J. Lories †‡*, S. Monteagudo †

† Laboratory of Tissue Homeostasis and Disease, Skeletal Biology and Engineering Research Center, KU Leuven, Leuven, Belgium

‡ Division of Rheumatology, University Hospitals Leuven, Leuven, Belgium



ARTICLE INFO

Article history:

Received 29 July 2018

Accepted 19 November 2018

Keywords:

Osteoarthritis

Cartilage

Epigenetics

DOT1L

DMM

Ageing

SUMMARY

Objective: We earlier identified that the histone methyltransferase Disruptor of telomeric silencing 1-like (DOT1L) is as a master protector of cartilage health via limiting excessive activation of the Wnt pathway. However, cartilage-specific homozygous *Dot1l* knockout mice exhibited a severe growth phenotype and perinatal death, which hampered their use in induced or ageing models of osteoarthritis (OA). The aim of this study was to generate and examine haploinsufficient and inducible conditional *Dot1l*-deficient mouse models to evaluate the importance of DOT1L during post-traumatic or ageing-associated OA onset and progression.

Method: We used cartilage-specific heterozygous and postnatal tamoxifen-inducible *Dot1l* knockout mice and performed destabilization of the medial meniscus (DMM) and ageing as OA models. Mice were examined histologically using X-rays and micro-computed tomography (μCT), and cartilage damage and osteophyte formation were assessed based on OARSI guidelines. Immunohistochemistry of DOT1L, H3K79me2, TCF1 and COLX was performed.

Results: Both *Dot1l*-deficient strains exhibit a phenotype characterized by joint remodeling with extensive osteophyte formation and ectopic ossification upon ageing, indicating accelerated development of spontaneous osteoarthritis. In the DMM-induced OA mouse model, absence of *Dot1l* resulted in increased cartilage damage. Wnt signalling hyper-activation and ectopic chondrocyte hypertrophy were observed in the articular cartilage of both *Dot1l*-deficient mice.

Conclusions: This study demonstrated the functional relevance of DOT1L *in vivo* during the development of OA using genetically modified mice. Thus, maintaining or enhancing DOT1L activity during ageing or after trauma might prevent OA onset and progression.

© 2018 Osteoarthritis Research Society International. Published by Elsevier Ltd. All rights reserved.

Introduction

Epigenetics refers to molecular mechanisms that control gene transcription and translation without changes in the underlying DNA sequence¹, and include histone modifications, DNA methylation and non-coding RNAs. Epigenetic processes maintain the specific cellular phenotype essential for the articular chondrocytes to ensure joint homeostasis, maintain tissue integrity and cope

with challenges such as tissue injury or ageing^{2–4}. Losing epigenetic control in the joint increases the susceptibility to develop osteoarthritis (OA)^{1,5,6}.

The Disruptor of telomeric silencing 1-like (DOT1L) gene encodes a histone methyltransferase that methylates lysine-79 of histone H3 (H3K79) and is involved in epigenetic regulation of gene transcription^{7–9}. Polymorphisms in *DOT1L* were associated with changes in hip cartilage thickness and OA^{10,11}. However, it was unknown how DOT1L affected this disease until we identified DOT1L as a master regulator of cartilage homeostasis¹². Pharmacological inhibition of DOT1L activity in human articular chondrocytes from healthy donors shifted their molecular signature towards an OA-like profile *in vitro*. *In vivo*, inhibition of DOT1L by intraarticular injection of DOT1L inhibitor in mice triggered OA. Mechanistically, DOT1L's protective role is accomplished via limiting Wnt signalling, a pathway that when hyper-activated leads

* Address correspondence and reprint requests to: R.J. Lories, Laboratory of Tissue Homeostasis and Disease, Skeletal Biology and Engineering Research Center, KU Leuven, Leuven, Belgium. Tel: 32-16-342542; Fax: 32-16-346200.

E-mail addresses: Frederique.Cornelis@kuleuven.be (F.M.F. Cornelis), Astrid.Deroover@student.kuleuven.be (A. de Roover), Lies.Storms@kuleuven.be (L. Storms), Ann.Hens@kuleuven.be (A. Hens), Rik.Lories@kuleuven.be (R.J. Lories), Silvia.Monteagudo@kuleuven.be (S. Monteagudo).

to joint disease^{13–15}. The Wnt cascade has been strongly linked to joint homeostasis and disease pathogenesis^{13,16}, but mechanisms controlling the level of Wnt activation are not fully understood.

In our previous study, homozygous deletion of *Dot1l* in chondrocytes (*Dot1l*^{CART-KO} mice) resulted in severe postnatal growth retardation and perinatal mortality¹². This precluded the use of *Dot1l*^{CART-KO} mice in post-traumatic or ageing models of OA, pointing out the need of creating new genetic mouse models to document the role of endogenous DOT1L in OA, thereby bypassing the use of pharmacological inhibitors with potential off-target effects. The purpose of this study was to generate and investigate haploinsufficient or inducible conditional mouse models of *Dot1l* gene deletion in articular cartilage, to study DOT1L in the development of spontaneous or post-traumatic OA. This will allow us to further understand the role of DOT1L in the onset and progression of OA, and to estimate the potential of targeting the DOT1L network for the treatment of this disease.

Materials and methods

Mice

Animal studies were approved by the Ethics Committee for Animal Research (P257-2015 and P159-2016; KU Leuven, Belgium). Mouse models are reported following ARRIVE guidelines (<https://www.nc3rs.org.uk/arrive-guidelines>) (Table 1). Mice were housed in groups of 4–5 in static micro-insulator cages with Macrolon filter and bedding material (composed of spruce particles of approximately 2.5–3.5 mm, type Lignocel® BK 8/15), under conventional conditions (14h light–10h dark; 23 ± 2°C), with standard chow food (Sniff, Soest, Germany) and water *ad libitum*. Wild-type C57Bl/6J mice were from Janvier (Le Genest St Isle, France). *Dot1l* transgenic mice (*Dot1l*^{tg}) were from the Knockout Mouse Project (KOMP) (CSD29070)¹⁷. Heterozygous mice were crossed to Gt(ROSA)26Sor^{tm1(FLP1)Dym} mice (Jax003946) for removal of the Stop-cassette, to obtain *Dot1l* mice in which exon 2 is flanked by *loxP* sites (*Dot1l*^{fl}). These mice were further bred to Tg(Col2a1.Cre) <1Bhr> mice (Jax003554)¹⁸, fully backcrossed to the CD1 background, to generate conditional heterozygous cartilage-specific *Dot1l* knockout mice (*Dot1l*^{fl/+};Col2-Cre^{+/−} or He *Dot1l*^{CART-KO}). Mice used in this study were in third generation backcross to C57Bl/6J. *Dot1l*^{fl/fl} were also bred to B6.Cg-Acan^{tm1(cre/ERT2)Crm}/J mice (Jax019148)¹⁹ (from Dr. G. Bou-Gharios and the Kennedy Institute, Oxford, UK) to generate inducible cartilage-specific *Dot1l* knockout mice (*Dot1l*^{fl/fl};Acan-Cre-ER^{+/−} or *Dot1l*^{CondCART-KO}). Mice used in this study were in second generation backcross to C57Bl/6J. Tamoxifen was injected at the age of 8 weeks (2 mg, 3 injections, every other day)¹⁹, to generate conditional cartilage-specific knockout mice. Genotypes of animals were confirmed by PCR upon weaning and after sacrifice¹².

Genotypes of animals were confirmed by PCR upon weaning and after sacrifice¹².

Osteoarthritis models

In the destabilization of the medial meniscus (DMM) mouse model of OA, mild instability of the knee was obtained by transection of the medial menisco-tibial ligament of the right knee²⁰. Arthritis was induced in male, 9-week old mice and knees were analyzed 12 weeks after surgery. Contra-lateral knee and sham surgery in wild-type mice served as control. Ageing heterozygous *Dot1l*^{CART-KO} mice were sacrificed at the age of 16 months, *Dot1l*-*CondCART-KO* mice in the DMM model at the age of 21 weeks and *Dot1l*^{CondCART-KO} mice in the ageing model at 12 months after

Table 1
Animal experiments: overview, set-up and analysis details

Experiment ID	Experiment details
1. 8-week old WT	* 8-week old male C57Bl/6J mice * Total sample size: n=3; WT: n=3
2. Ageing model of OA in WT	* Primary outcome: IHC detection of protein expression: Fig. 1A and B * 12-month old female C57Bl/6J mice * Total sample size: n=3; WT: n=3
3. DMM model of OA in WT	* Primary outcome: IHC detection of protein expression: Fig. 1A and B * 20-week old male C57Bl/6J mice (time of sacrifice - induction of model at 8 weeks) * Total sample size: n=6; WT SHAM: n=3, WT DMM: n=3
4. Ageing model of OA in heterozygous <i>Dot1l</i> ^{CART-KO}	* Primary outcome: IHC detection of protein expression: Fig. 1C and D * 16-month old male heterozygous <i>Dot1l</i> ^{CART-KO} and control mice * controls: <i>Dot1l</i> ^{fl/+} ;Col2-Cre ^{−/−} : n=1, <i>Dot1l</i> ^{fl/+} ;Acan-Cre-ER ^{+/−} no tamoxifen: n=2, <i>Dot1l</i> ^{fl/+} ;Acan-Cre-ER ^{−/−} : n=2, C57Bl/6J: n=1 * Total sample size: n=8; He <i>Dot1l</i> ^{CART-KO} : n=3, Control: n=5 * Primary outcome: imaging: X-rays and μCT: Fig. 2D and E * Primary outcome: histology and scoring: Figs. 2F and 3A–C * Secondary outcome: IHC detection of protein expression: Figs. 2(B and C) and 3(D and E)
5. 12-week old <i>Dot1l</i> ^{CondCART-KO}	* 12-week old male <i>Dot1l</i> ^{CondCART-KO} and control mice * controls: <i>Dot1l</i> ^{fl/fl} ;Acan-Cre-ER ^{−/−} no tamoxifen * Total sample size: n=6; <i>Dot1l</i> ^{CondCART-KO} : n=3, Control: n=3 * Primary outcome: IHC detection of protein expression: Fig. 4B and C
6. DMM model of OA in <i>Dot1l</i> ^{CondCART-KO}	* 21-week old male <i>Dot1l</i> ^{CondCART-KO} and control mice (time of sacrifice - induction of model at 9 weeks) * controls: pooled from <i>Dot1l</i> ^{fl/fl} ;Acan-Cre-ER ^{+/−} + oil; <i>Dot1l</i> ^{fl/fl} ;Acan-Cre-ER ^{−/−} + tamoxifen and <i>Dot1l</i> ^{fl/fl} ;Acan-Cre-ER ^{−/−} + oil groups * Total sample size: n=38; <i>Dot1l</i> ^{CondCART-KO} : n=20, Control: n=18 * Primary outcome: histology and scoring: Fig. 5B–D * Secondary outcome: IHC detection of protein expression: Fig. 5E and F
7. Ageing model of OA in <i>Dot1l</i> ^{CondCART-KO}	* 14-month old male <i>Dot1l</i> ^{CondCART-KO} and control mice * controls: pooled from <i>Dot1l</i> ^{fl/fl} ;Acan-Cre-ER ^{+/−} + oil; <i>Dot1l</i> ^{fl/fl} ;Acan-Cre-ER ^{−/−} + tamoxifen and <i>Dot1l</i> ^{fl/fl} ;Acan-Cre-ER ^{−/−} + oil groups * Total sample size: n=19; <i>Dot1l</i> ^{CondCART-KO} : n=6, Control: n=13 * Primary outcome: imaging: X-rays and μCT: Fig. 6B,C and E * Primary outcome: histology and scoring: Figs. 6D and 7A–C * Secondary outcome: IHC detection of protein expression: Fig. 7D and E

Abbreviations: ID, identity; WT, wild-type; IHC, immunohistochemistry; OA, osteoarthritis; DMM, destabilization of the medial meniscus; KO, knockout; He, heterozygous; μCT, micro-computed tomography.

tamoxifen injections (14 months of age). Control animals in the conditional knockout experiments (DMM model and ageing model) were pooled from *Dot1l*^{f/f};Acan-Cre-ER^{+/−}+oil; *Dot1l*^{f/f};Acan-Cre-ER^{+/−}+tamoxifen and *Dot1l*^{f/f};Acan-Cre-ER^{+/−}+oil groups. Four control animals injected with oil, in the DMM model experiment, were exposed to tamoxifen by the stool resulting in effective recombination and were therefore allocated to the conditional knockout group. Two animals were excluded in the *Dot1l*^{CondCART-KO} ageing group as correct genotype post-tamoxifen exposure could not be established.

Histology

Dissected mouse knees were fixed overnight at 4°C in 2% Formaldehyde, decalcified for 3 weeks in 0.5M EDTA pH 7.5, and embedded in paraffin. Hematoxylin-safraninO staining, toluidine blue staining and immunohistochemistry were performed on 5 µm thick sections. Severity of disease was determined by histological scores on hematoxylin-safraninO stained sections throughout the knee (10 sections at 100 µm distance). Cartilage damage was assessed based on OARSI guidelines²¹. Depth of lesion (0–6) was scored on frontal knee sections. The score represents the max score for the ageing heterozygous *Dot1l*^{CART-KO} mice or the mean score in *Dot1l*^{CondCART-KO} mice, at the medial tibia. A scoring system for osteophytes was developed. The presence and size of osteophytes were quantified at the four quadrants in heterozygous *Dot1l*^{CART-KO} mice or at the medial tibia in *Dot1l*^{CondCART-KO} mice. Scoring grades represent the following features; 0: no osteophytes; 0.5: possible small osteophyte; 1: definite small osteophyte, 2: medium osteophyte, 3: large and mature osteophyte. Scoring was done by two independent readers, blinded to the genotype. Pictures were taken using a Visitron Systems microscope (Leica Microsystems GmbH) using Spot32 software.

Immunohistochemistry

Immunohistochemistry was performed on paraffin-embedded EDTA-decalcified knee sections. Heat induced epitope retrieval was performed using a Citrate-EDTA buffer (pH 6.2) for 10 min at 98°C, except for the detection of DOT1L. Sections were treated with 3% H₂O₂/methanol for 10 min to inactivate endogenous peroxidase, blocked in goat serum for 30 min and incubated overnight at 4°C with primary antibodies against DOT1L (Abcam, ab64077), COLX (Abcam, ab58632), TCF1 (Abcam, ab96777) or for 90 min with primary antibody against H3K79me2 (Abcam, ab3594). Rabbit IgG (Santa Cruz, sc-2027) was used as negative control. Avidin-biotin complex amplification (Vectastain ABC kit, Vector Laboratories, USA) was used, except for the immunohistochemical detection of DOT1L and H3K79me2. Peroxidase goat anti-rabbit IgG (Jackson Immunoresearch, Suffolk, UK) was applied for 30 min and peroxidase activity was determined using DAB. For detection of COLX, antigen retrieval was performed as reported¹². Quantification of the DAB staining was performed with color deconvolution plugin (Jacqui Ross, Auckland University) in ImageJ Software (NIH Image, National Institutes of Health). Quantification was performed using two technical replicates for three different mice per condition in separate experiments²², with staining intensity reported relative to the control mice in the same experiment.

µCT 3D reconstruction

Mice were scanned by *in vivo* small animal micro-computed tomography (µCT) (SkyScan1076, software version 3.2, Kontich, Belgium). Image parameters were 50 kVp X-ray source voltage,

100 µA current, a composite X-ray filter of 1 mm aluminium, acquiring projections with 1° increments over an angle of 180°, images with a real pixel size of 9 µm. Tomograms were reconstructed using Nrecon software (version 1.6.1.3, SkyScan) and 3D reconstructions generated using CTvox software (version 3.3.0, SkyScan).

X-rays

Full body X-rays of mice were made using a Direct Radiography model DM 100 Embrace mammography (Hologic, Agfa Gevaert, Mortsel, Belgium).

Statistical analysis

Data in the graphs are distinct data points obtained from the analysis of individual mice. For statistical analyses and graphs, R Studio (Version 1.0.15) and GraphPad Prism (Version 5) were used. For disease severity scores (OARSI grade for cartilage damage and osteophyte score), normal distribution was assumed based on the score's parameter characteristics in mice that are over 80% genetically identical. The normality assumption was further evaluated by visual inspection of QQ plots and by Shapiro–Wilk normality tests. *T*-tests were applied taking into account equal variances (as compared by the Levene test). 95% confidence intervals (CI) of the difference between the means were calculated. For immunohistochemistry analysis, one-group *t*-test was used²². When normal distribution could not be assumed based on the evaluation above, which was only the case for the spontaneously occurring OA in ageing *Dot1l*^{CondCART-KO} mice, Mann–Whitney test was performed. *P*-values less than 0.05 were considered significant.

Results

DOT1L activity is decreased in osteoarthritis mouse articular cartilage

We previously reported that, in humans, DOT1L activity is positively associated with cartilage health¹². DOT1L activity, assessed by the levels of H3K79 di-methylation, was decreased in cartilage from OA patients compared to non-OA patients¹². Here, we investigated whether DOT1L activity is similarly decreased in mouse models of ageing and post-traumatic OA. Twelve-month old C57Bl/6J mice spontaneously develop mild OA, mostly characterised by surface fibrillations and small fissures of the cartilage²³. We performed immunohistochemical staining of DOT1L and di-methylated H3K79 on articular cartilage from knees of 12-month old compared to 8-week old mice [Fig. 1(A and B)]. The immunoreactive signal of DOT1L [discrepancy −90.04; *t*(2) = 37.64, *P* = 0.0007, 95%CI of discrepancy = (−100.3–(−79.75))] and di-methylated H3K79 [discrepancy −83.04; *t*(2) = 38.43, *P* = 0.0007, 95%CI of discrepancy = (−92.33–(−73.74))] was decreased in cartilage of aged compared to young mice. Further, we assessed the levels of DOT1L and H3K79 di-methylation in cartilage from knees of mice with DMM-induced OA compared to sham-operated mice [Fig. 1(C and D)]. Likewise, the DOT1L [discrepancy −83.05; *t*(2) = 22.14, *P* = 0.0020, 95%CI of discrepancy = (−99.19–(−66.91))] and di-methylated H3K79 [discrepancy −86.41; *t*(2) = 40.44, *P* = 0.0006, 95%CI of discrepancy = (−95.6–(−77.22))] immunoreactive signal was diminished in the cartilage from mice with DMM-triggered OA compared to sham-operated mice. These observations demonstrate that, similarly to human OA, DOT1L activity is reduced in mouse OA cartilage, in both ageing and post-traumatic models of the disease.

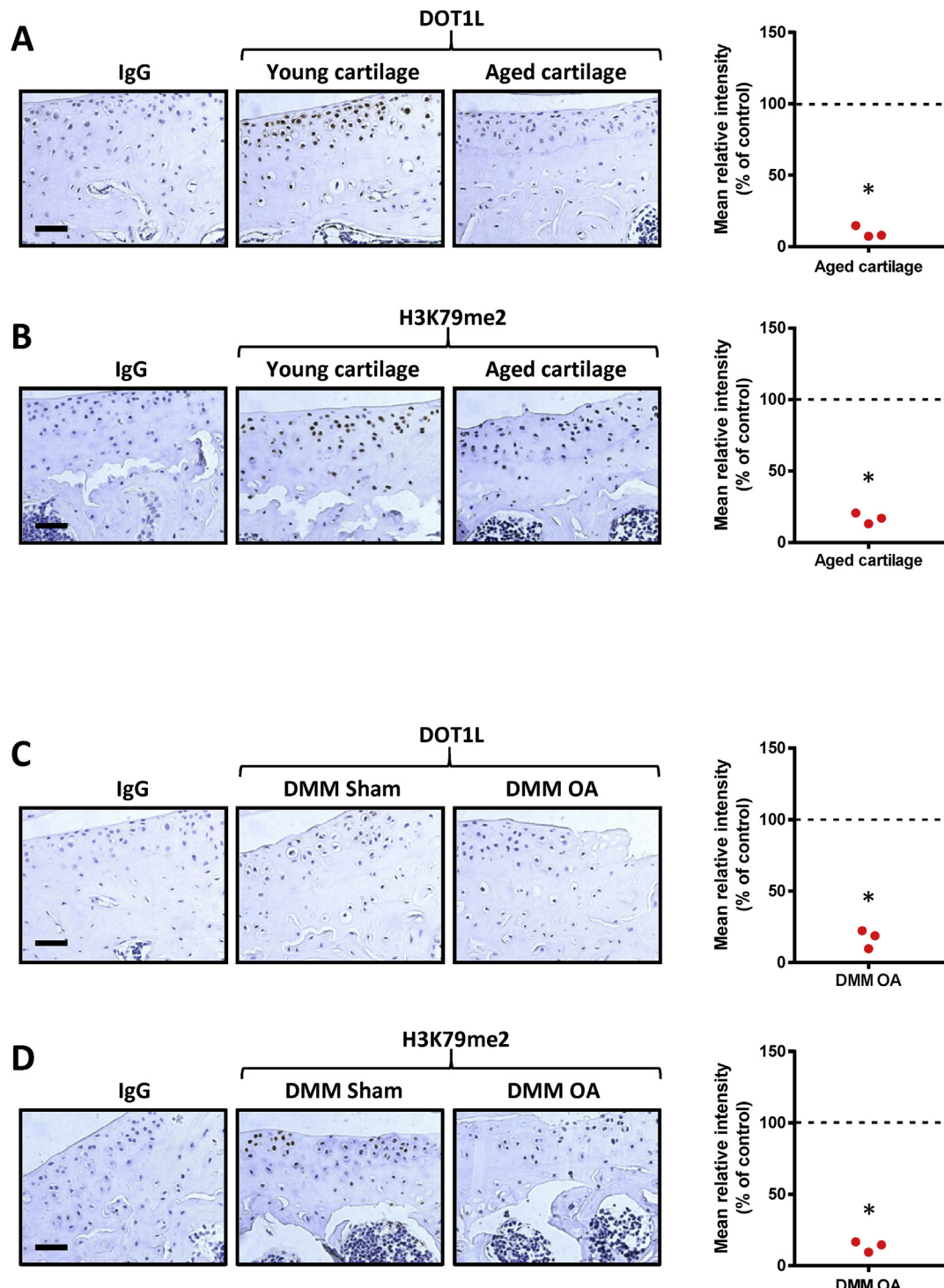


Fig. 1. DOT1L levels and activity are decreased in the articular cartilage of aged mice and of mice with OA triggered by destabilization of the medial meniscus (DMM) surgery. (A–B) Immunohistochemical detection and quantification of DOT1L levels [discrepancy -90.04 ; $t(2) = 37.64$, $*P = 0.0007$, 95%CI of discrepancy $= (-100.3 - (-79.75))$] and H3K79 di-methylation levels [discrepancy -83.04 ; $t(2) = 38.43$, $*P = 0.0007$, 95%CI of discrepancy $= (-92.33 - (-73.74))$] in the articular cartilage of the medial tibia of wild-type female aged mice (12-month old) compared to young male mice (8-week old). (C–D) Immunohistochemical detection and quantification of DOT1L levels [discrepancy -83.05 ; $t(2) = 22.14$, $*P = 0.0020$, 95%CI of discrepancy $= (-99.19 - (-66.91))$] and H3K79 di-methylation levels [discrepancy -86.41 ; $t(2) = 40.44$, $*P = 0.0006$, 95%CI of discrepancy $= (-95.6 - (-77.22))$] in the articular cartilage of wild-type male mice with OA triggered by DMM surgery compared to sham operated mice. (A–D) Data are presented as individual data points. The images are representative of three different animals. Scale bar: $50 \mu\text{m}$.

Heterozygous *Dot1l*^{CART-KO} mice display ectopic ossification

To study the impact of reduced DOT1L function in cartilage, we used cartilage-specific heterozygous *Dot1l* knockout mice and evaluated the effects of the haploinsufficiency. We bred

heterozygous floxed *Dot1l* mice (*Dot1l*^{f/+}) with a *Col2-Cre* deleter mouse strain (*Col2-Cre*^{+/−})¹⁸ to obtain specific recombination in chondrocytes (*Dot1l*^{f/+}; *Col2-Cre*^{+/−}) (heterozygous (He) *Dot1l*^{CART-KO}), and mice were aged till 16 months [Fig. 2(A)]. To evaluate DOT1L levels and activity in the articular cartilage from

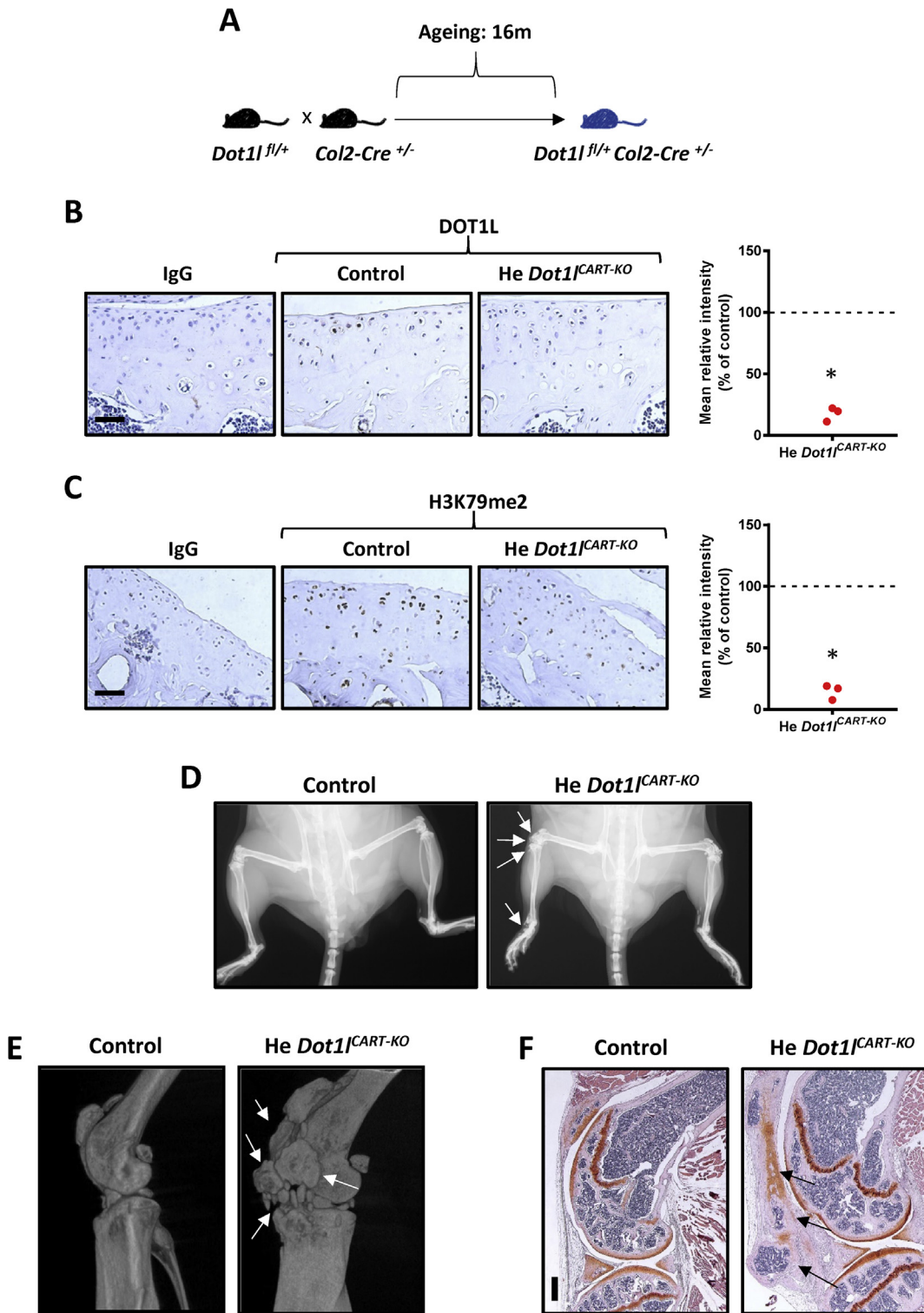


Fig. 2. Heterozygous male *Dot1l*^{CART-KO} mice spontaneously develop ectopic bone formation by the age of 16 months. (A) Schematic outline of the heterozygous *Dot1l*^{CART-KO} (*Dot1l*^{f/f} *Col2-Cre*^{+/−}) spontaneous mouse model. (B–C) Immunohistochemical detection and quantification of DOT1L levels [discrepancy -82.28 ; $t(2) = 24.88$, $*P = 0.0016$, 95%CI of discrepancy $= (-96.51 - (-68.05))$] and H3K79 di-methylation levels [discrepancy -85.4 ; $t(2) = 24.37$, $*P = 0.0017$, 95%CI of discrepancy $= (-100.5 - (-70.32))$] in the articular cartilage of the medial tibia in 16-month old male heterozygous *Dot1l*^{CART-KO} mice compared to control animals. Data are presented as individual data points. The images are representative of three different animals in each group. Scale bar: 50 μ m. (D) X-ray images of the hind limbs of 16-month old male heterozygous *Dot1l*^{CART-KO} and control mice. (E) Three-dimensional reconstruction of a micro-computed tomography (μCT) of the right knee of a 16-month old male heterozygous *Dot1l*^{CART-KO} and control mouse and (F) hematoxylin-safranin O staining of the same knee (sagittal view). Scale bar: 500 μ m. (D–F) The images are representative of three heterozygous *Dot1l*^{CART-KO} mice and five control mice and arrows point at ectopic bone formation.

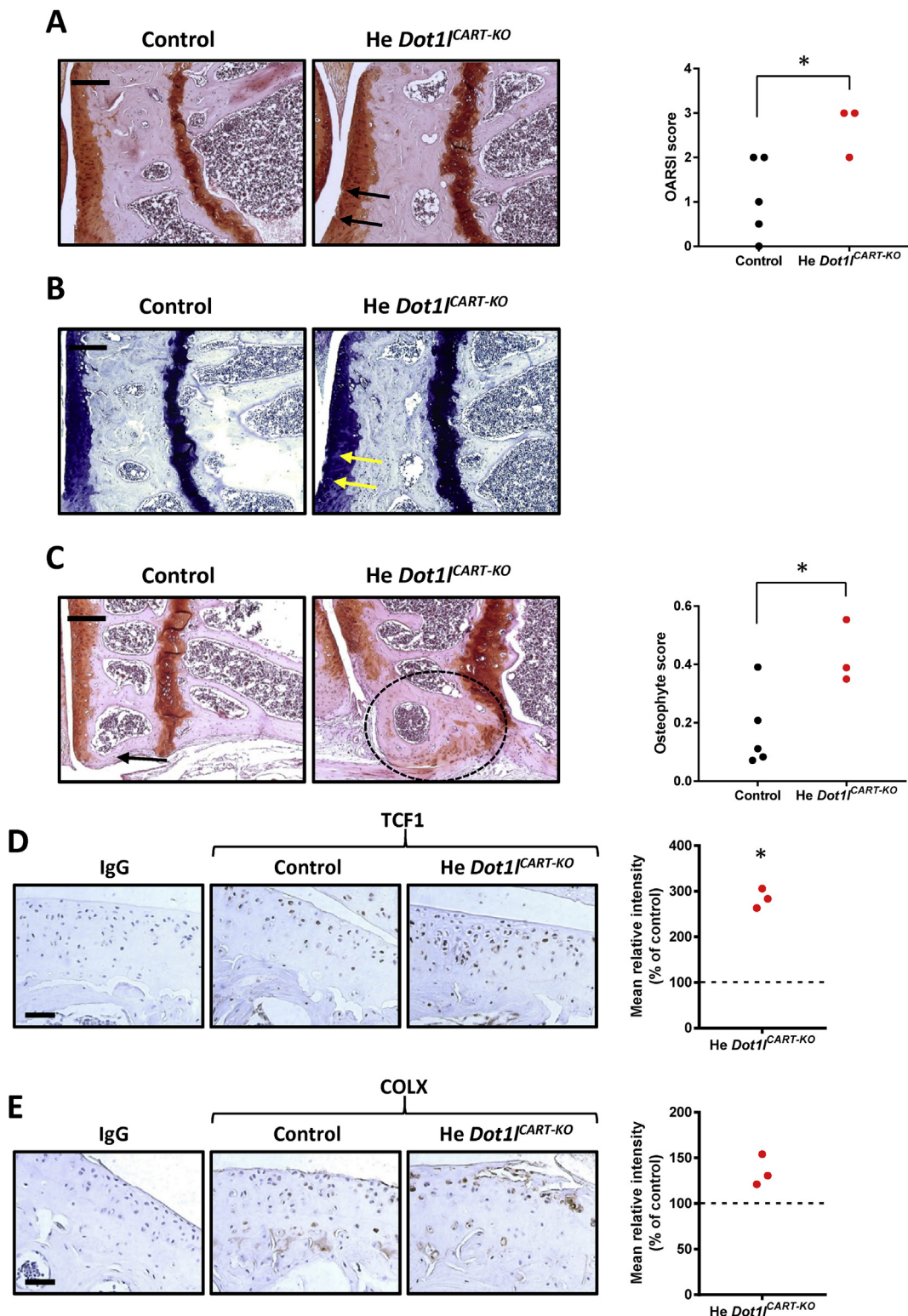


Fig. 3. Heterozygous male *Dot1l*^{CART-KO} mice spontaneously develop osteoarthritis by the age of 16 months. (A) Frontal hematoxylin-safraninO staining of the medial tibia and quantification of articular cartilage damage at the medial tibia, evaluated by OARSI score. Data are presented as individual data points [$t(6) = 2.672$, $^*P = 0.037$; 95%CI difference between the means = (0.132–3.001)]. (B) Frontal toluidine blue staining of the medial tibia. (A–B) Arrows point at cartilage lesions. (C) Frontal hematoxylin-safraninO staining of the lateral tibia and quantification of osteophytes at the four quadrants. Data are presented as individual data points [$t(6) = 2.819$, $^*P = 0.030$, 95%CI of difference between the means = (0.0340–0.482)]. The arrow points at a small osteophyte, the circle indicates a large osteophyte. (A–C) The images are representative of three heterozygous *Dot1l*^{CART-KO} mice and five control mice. Scale bar: 200 μ m. Immunohistochemical detection and quantification of TCF1 [discrepancy 184.2; $t(2) = 14.96$, $^*P = 0.0044$, 95%CI of discrepancy = (131.2–237.1)] (D) and COLX [discrepancy 35.25; $t(2) = 3.606$, $P = 0.0691$, 95%CI of discrepancy = (−6.815–77.31)] (E) in the articular cartilage of the medial tibia of male heterozygous *Dot1l*^{CART-KO} and control mice. (D–E) The images are representative of three heterozygous and 3 control mice and data are presented as individual data points. Scale bar: 50 μ m.

heterozygous *Dot1l*^{CART-KO} compared to control mice, we performed immunohistochemistry for DOT1L and di-methylated H3K79 [Fig. 2(B and C)]. We confirmed that the immunoreactive signal of DOT1L [discrepancy -82.28 ; $t(2) = 24.88$, $P = 0.0016$, 95%CI of discrepancy $= (-96.51 - (-68.05))$] and di-methylated H3K79 [discrepancy -85.4 ; $t(2) = 24.37$, $P = 0.0017$, 95%CI of discrepancy $= (-100.5 - (-70.32))$] was decreased in the articular cartilage of heterozygous *Dot1l*^{CART-KO} mice compared to control cartilage.

At 16 months, we observed that heterozygous *Dot1l*^{CART-KO} mice had difficulties bending their knees. X-rays of the hind limbs [Fig. 2(D)] revealed extensive ectopic bone formation in knees and ankles of heterozygous *Dot1l*^{CART-KO} mice. Three-dimensional μ -CT reconstruction of the knee performed at the same time point [Fig. 2(E)] and histological analysis [Fig. 2(F)] confirmed ectopic bone formation in heterozygous *Dot1l*^{CART-KO} mice. Ectopic bone mostly seemed to be localised in osteophytes and in the joint's soft tissues, like ligaments and the synovium.

Heterozygous *Dot1l*^{CART-KO} mice develop spontaneous osteoarthritis

To assess the development of spontaneous articular cartilage damage in heterozygous *Dot1l*^{CART-KO} mice, disease severity was scored following OARSI guidelines²¹ [Fig. 3(A)]. This revealed that, upon ageing, haploinsufficient mice develop more cartilage

damage than control mice [mean score 2.66 vs 1.1; $t(6) = 2.672$, $P = 0.037$; 95%CI difference between the means $= (0.132 - 3.001)$]. Proteoglycan content, further assessed by toluidine blue staining, confirmed the OARSI scores [Fig. 3(B)]. Additionally, we evaluated the presence of osteophytes on sections of the knee joint [Fig. 3(C)]. Heterozygous *Dot1l*^{CART-KO} mice displayed significantly more osteophyte formation compared to control mice [mean score 0.431 vs 0.173; $t(6) = 2.819$, $P = 0.030$, 95%CI of difference between the means $= (0.0340 - 0.4817)$]. Hence, heterozygous *Dot1l*^{CART-KO} mice develop more severe spontaneous OA upon ageing compared to control mice.

Heterozygous *Dot1l*^{CART-KO} mice display increased Wnt signalling and chondrocyte hypertrophy in the articular cartilage

Then, to evaluate Wnt pathway activity in the articular cartilage of these mice, we performed immunohistochemical detection of TCF1, a Wnt target gene directly dependent on DOT1L transcriptional regulation¹² [Fig. 3(D)]. We observed increased protein expression of TCF1 in the articular cartilage of heterozygous *Dot1l*^{CART-KO} mice compared to controls [discrepancy 184.2; $t(2) = 14.96$, $P = 0.0044$, 95%CI of discrepancy $= (131.2 - 237.1)$], suggesting hyper-activation of the Wnt pathway in haploinsufficient mice.

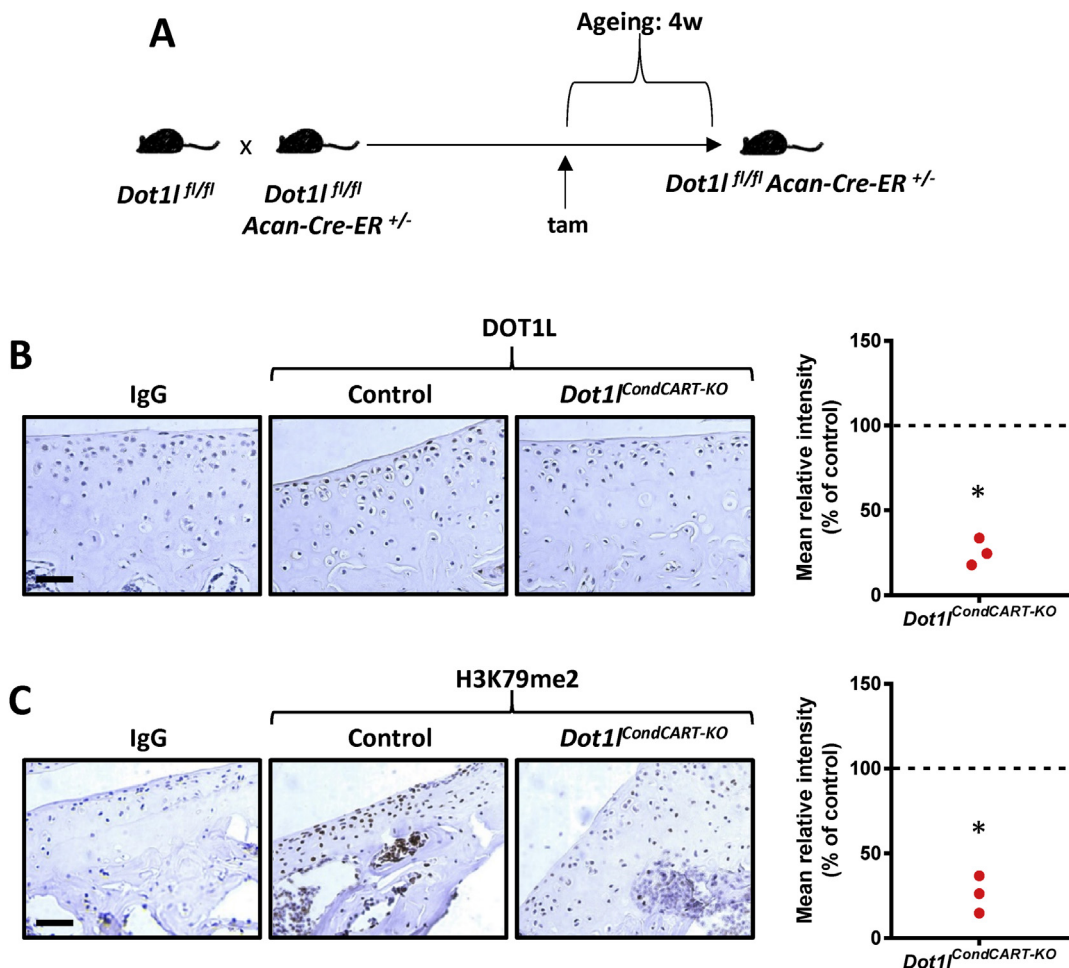


Fig. 4. Postnatal deletion of *Dot1l* results in decreased DOT1L and H3K79 di-methylation levels in the articular cartilage. (A) Schematic outline of the postnatal deletion of *Dot1l* in the *Dot1l*^{CondCART-KO} mouse model (*Dot1l*^{fl/fl} - *Acan-Cre-ER*^{+/−}). (B–C) Immunohistochemical detection and quantification of DOT1L levels [discrepancy -74.56 ; $t(2) = 16.21$, $*P = 0.0038$, 95%CI of discrepancy $= (-94.35 - (-54.77))$] and H3K79 di-methylation [discrepancy -74.04 ; $t(2) = 11.67$, $*P = 0.0073$, 95%CI of discrepancy $= (-101.3 - (-46.74))$] in the articular cartilage of the medial tibia in male 12-week old *Dot1l*^{CondCART-KO} mice compared to control animals. Data are presented as individual data points. The images are representative of three *Dot1l*^{CondCART-KO} mice and three control mice. Scale bar: 50 μ m.

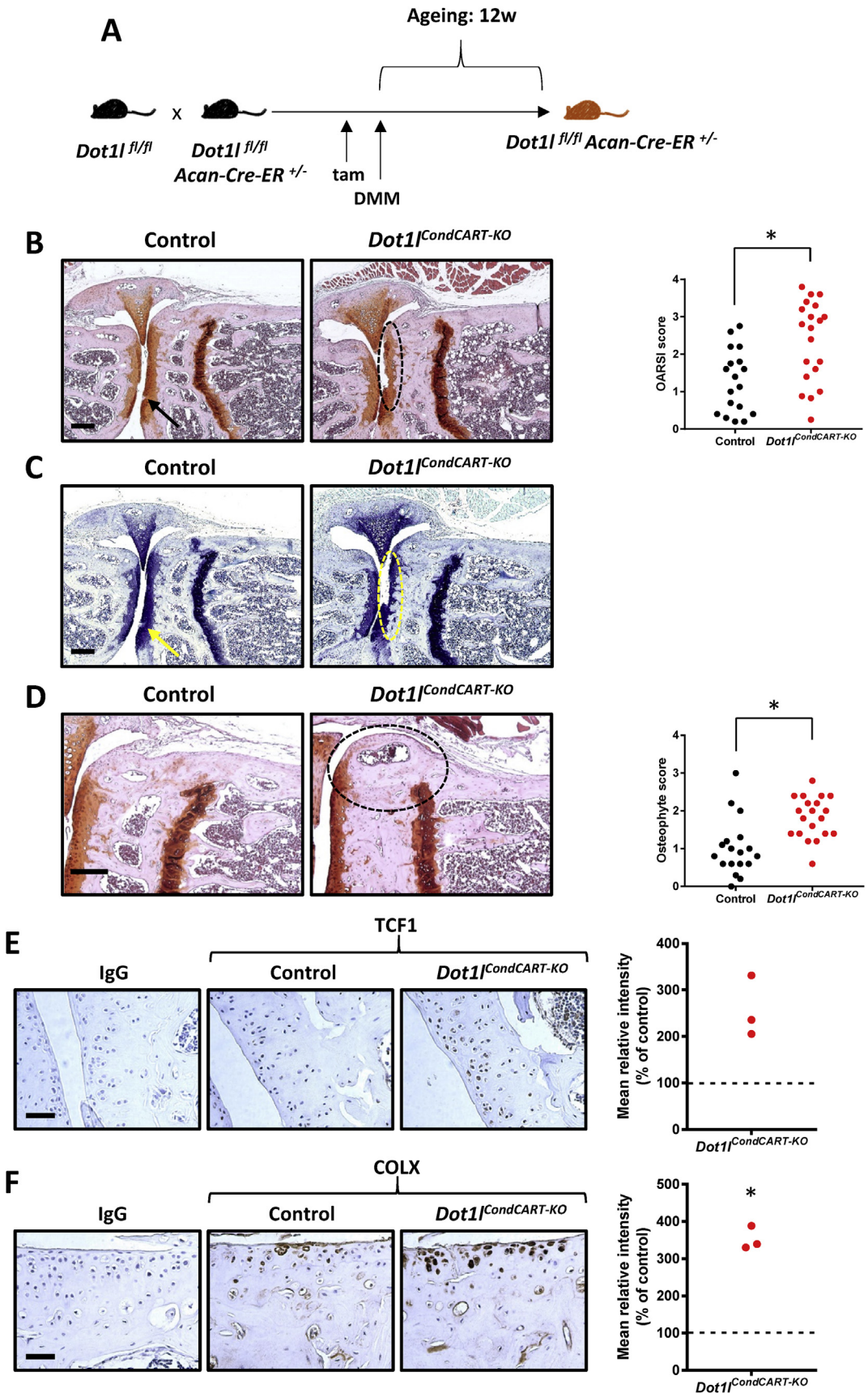


Fig. 5. Postnatal male $Dot1l^{CondCART-KO}$ mice develop severe post-traumatic osteoarthritis after DMM. (A) Schematic outline of the postnatal $Dot1l^{CondCART-KO}$ DMM osteoarthritis mouse model ($Dot1l^{fl/fl}$ - $Acan-Cre-ER^{+/+}$). (B) Frontal hematoxylin-safraninO staining of the medial condyles and quantification of articular cartilage damage at the medial tibia, evaluated by the OARSI scoring system, in the $Dot1l^{CondCART-KO}$ DMM mice. Data are presented as individual data points [$t(36) = 3.455$, $^*P = 0.0014$, 95%CI of differences between the

In OA, articular chondrocytes lose their stable molecular identity and differentiate towards hypertrophic chondrocytes, a process that contributes to cartilage degradation and that has been associated with increased Wnt signalling^{24,25}. To determine the presence of hypertrophic chondrocytes in the articular cartilage of heterozygous *Dot1l*^{CART-KO} mice, immunohistochemistry for chondrocyte hypertrophy marker collagen type 10 (COLX) was performed [Fig. 3(E)]. This analysis suggested increased COLX protein levels in the articular cartilage of heterozygous *Dot1l*-deficient mice compared to controls [discrepancy 35.25; $t(2) = 3.606, P = 0.0691$, 95%CI of discrepancy = (−6.815–77.31)].

Postnatal tamoxifen-induced conditional *Dot1l*^{CART-KO} mice develop severe post-traumatic osteoarthritis

To study the impact of the postnatal deletion of *Dot1l* in mouse cartilage, we bred homozygous floxed *Dot1l* mice (*Dot1l*^{fl/fl}) with an *Acan-Cre-ER* mouse strain (*Acan-Cre-ER*^{+/−})¹⁹ to obtain postnatal tamoxifen-inducible specific recombination in chondrocytes (*Dot1l*^{fl/fl}; *Acan-Cre-ER*^{+/−}) (*Dot1l*^{CondCART-KO}). To induce recombination, mice were injected with tamoxifen at the age of 8 weeks¹⁹ [Fig. 4(A)]. We first studied DOT1L levels and activity in *Dot1l*^{CondCART-KO} mice, by immunohistochemistry of DOT1L and H3K79 di-methylation on knee articular cartilage from *Dot1l*^{CondCART-KO} mice and control mice at the age of 12 weeks [Fig. 4(B and C)]. DOT1L levels [discrepancy −74.56; $t(2) = 16.21, P = 0.0038$, 95%CI of discrepancy = (−94.35 – (−54.77))] and dimethylated H3K79 levels [discrepancy −74.04; $t(2) = 11.67, P = 0.0073$, 95%CI of discrepancy = (−101.3 – (−46.74))] were strongly reduced in the articular cartilage of *Dot1l*^{CondCART-KO} mice compared to control cartilage, validating the efficiency of the knockout technique.

To study whether postnatal *Dot1l*^{CondCART-KO} mice develop more severe post-traumatic OA, we performed DMM surgery in the right knee of these mice and in control mice at the age of 9 weeks [Fig. 5(A)]. Disease severity was scored following OARSI guidelines²¹ [Fig. 5(B)]. *Dot1l*^{CondCART-KO} mice display significantly more severe cartilage damage than controls upon DMM surgery [mean score 2.363 vs 1.268; $t(36) = 3.455, P = 0.001$, 95%CI of differences between the means = (0.452–1.737)]. Toluidine blue staining confirmed the OARSI score data [Fig. 5(C)]. In addition, we quantified the presence of osteophytes on knee sections [Fig. 5(D)]. We observed more osteophyte formation in *Dot1l*^{CondCART-KO} mice compared to controls upon DMM surgery [mean score 1.83 vs 1.011; $t(36) = 3.887, P < 0.001$, 95%CI of differences between the means = (0.3916–1.246)]. Thus, *Dot1l*^{CondCART-KO} mice develop severe post-traumatic OA after joint injury.

Immunohistochemistry analysis of TCF1 suggested increased activation of the Wnt pathway in the articular cartilage of *Dot1l*^{CondCART-KO} mice compared to controls upon DMM surgery [discrepancy 157.6; $t(2) = 4.157, P = 0.0533$, 95%CI of discrepancy = (−5.509–320.7)] [Fig. 5(E)]. We also observed enhanced chondrocyte hypertrophy by immunohistochemistry of COLX, in the articular cartilage of these mutant mice compared to controls, upon DMM surgery [discrepancy 252.7; $t(2) = 14, P = 0.0051$, 95%CI of discrepancy = (175–330.4)] [Fig. 5(F)].

Postnatal tamoxifen-induced conditional *Dot1l*^{CART-KO} mice display ectopic ossification and develop spontaneous osteoarthritis upon ageing

Next, to investigate the development of spontaneous OA upon ageing, *Dot1l*^{fl/fl}; *Acan-Cre-ER*^{+/−} mice were injected with tamoxifen at the age of 8 weeks to induce recombination (*Dot1l*^{CondCART-KO}), and mice were aged for another 52 weeks (until the age of 14 months) [Fig. 6(A)]. X-Ray images of the hind limbs [Fig. 6(B)], μCT three-dimensional reconstructions of the right knee [Fig. 6(C)] and histological analysis of the knees [Fig. 6(D)], at 52 weeks after tamoxifen injection, clearly showed ectopic bone formation in tamoxifen-induced *Dot1l*^{CondCART-KO} mice. Three-dimensional reconstruction of μ-CT images of the same knee within an individual *Dot1l*^{CondCART-KO} mouse at different time points after tamoxifen injection [Fig. 6(E)], illustrates the evolution of the ectopic bone formation over time.

Then, we studied the development of spontaneous cartilage damage upon ageing in *Dot1l*^{CondCART-KO} mice compared to controls. Disease severity was scored following OARSI guidelines²¹ [Fig. 7(A)]. Upon ageing, *Dot1l*^{CondCART-KO} mice display more cartilage damage than controls (median score 0.679 vs 0.2; $U = 9.5, P = 0.007$). Proteoglycan content, determined by toluidine blue staining, was more reduced at areas of cartilage lesions in *Dot1l*^{CondCART-KO} mice than in controls [Fig. 7(B)]. We also observed that aged *Dot1l*^{CondCART-KO} mice develop more osteophyte formation than controls [Fig. 7(C)] (median 1.982 vs 0; $U = 2, P < 0.001$). Altogether, *Dot1l*^{CondCART-KO} mice develop more severe OA upon ageing.

Mechanistically, we demonstrated again increased Wnt pathway activity in the articular cartilage of *Dot1l*^{CondCART-KO} mice upon ageing, compared to control mice [discrepancy 239.4; $t(2) = 10.82, P = 0.0084$, 95%CI of discrepancy = (144.2–334.7)] [Fig. 7(D)]. Immunohistochemical analysis of COLX suggested enhanced chondrocyte hypertrophy in the articular cartilage of the *Dot1l*^{CondCART-KO} mice upon ageing [discrepancy 284; $t(2) = 3.762, P = 0.0639$, 95%CI of discrepancy = (−40.8–608.9)] [Fig. 7(E)].

Discussion

We previously identified that histone methyltransferase DOT1L is a key protector of cartilage homeostasis, using human articular chondrocytes and a pharmacological DOT1L inhibition approach in mice¹². However, *in vivo* assessment of these insights using genetic mouse models to establish the impact of *Dot1l* loss of function in the development of OA, was missing. Homozygous *Dot1l*^{CART-KO} mice generated in this previous study had severe growth retardation and died around 4 weeks of age. Here, we generated haploinsufficient and inducible postnatal *Dot1l*-deficient mouse models, and investigated the joint phenotype of these mice upon ageing and joint injury. We also examined whether hyperactivation of Wnt signalling and chondrocyte hypertrophy occur in the articular cartilage of these new *Dot1l*-deficient strains.

OA is strongly linked to ageing but the mechanisms for this link are insufficiently understood²⁶. Upon ageing, both heterozygous *Dot1l*^{CART-KO} mice and postnatal tamoxifen-induced *Dot1l*^{CondCART-KO}

means = (0.452–1.737). (C) Toluidine blue staining of the medial condyles. (B–C) The arrow points at a small cartilage lesion and the circle indicates a large cartilage lesion. Scale bar: 250 μm. (D) Frontal hematoxylin–safraninO stained sections of the medial tibia and quantification of the presence of osteophytes at the medial tibia in the tamoxifen-induced *Dot1l*^{CondCART-KO} DMM mice. Data are presented as individual data points [$t(36) = 3.887, *P = 0.0004$, 95%CI of differences between the means = (0.3916–1.246)]. The circle emphasizes an osteophyte. Scale bar: 200 μm. (B–D) Tamoxifen-induced *Dot1l*^{CondCART-KO} DMM $n = 20$, control $n = 18$. Immunohistochemical detection and quantification of TCF1 [discrepancy 157.6; $t(2) = 4.157, P = 0.0533$, 95%CI of discrepancy = (−5.509–320.7)] (E) and COLX [discrepancy 252.7; $t(2) = 14, *P = 0.0051$, 95%CI of discrepancy = (175–330.4)] (F) in the articular cartilage of the medial tibia of *Dot1l*^{CondCART-KO} mice and control mice. (E–F) Data are presented as individual data points and the images are representative of three *Dot1l*^{CondCART-KO} mice and three control mice. Scale bar: 50 μm.

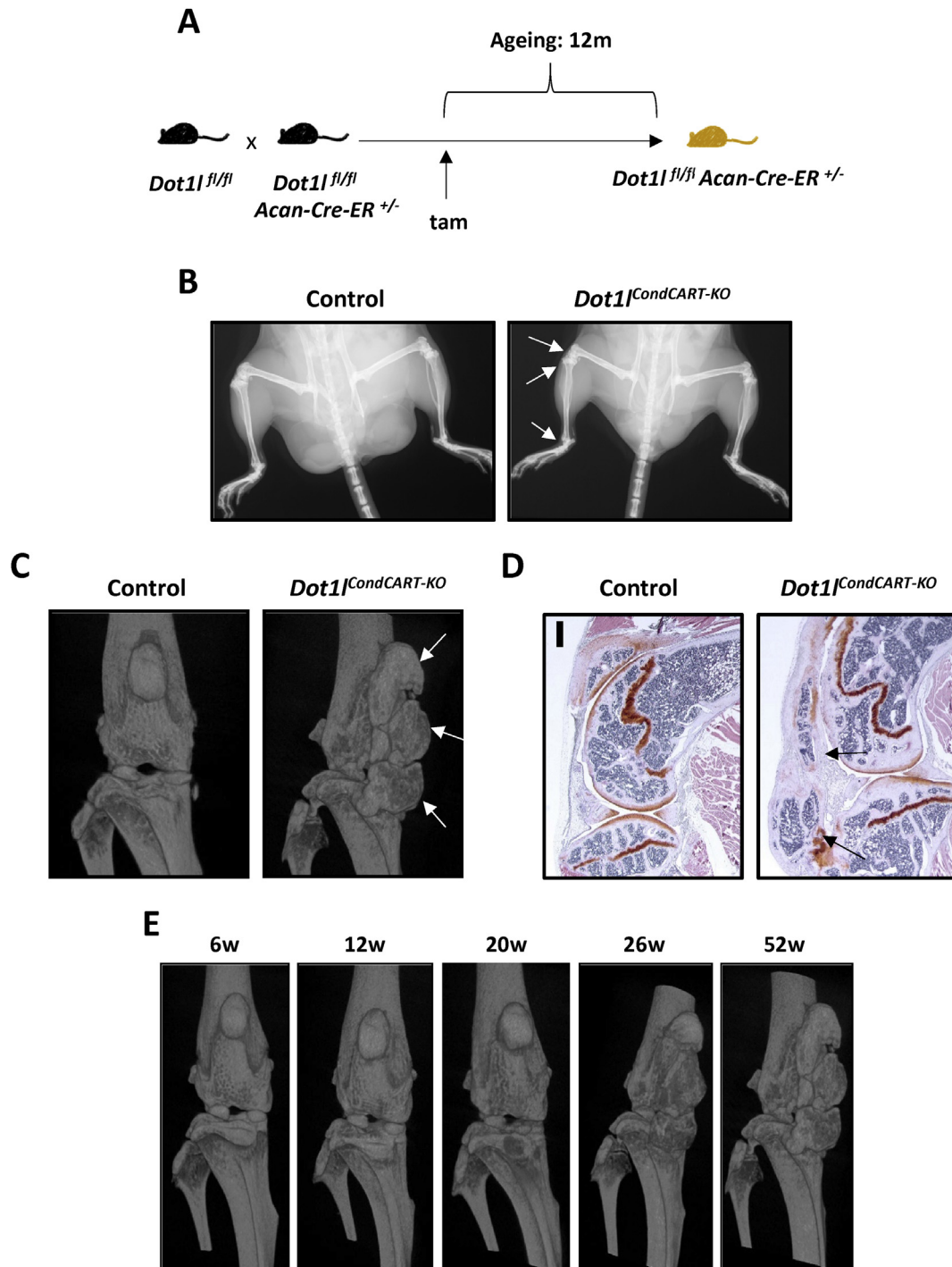


Fig. 6. Postnatal male *Dot1l*^{CondCART-KO} mice spontaneously develop ectopic bone formation by the age of 14 months. (A) Schematic outline of the postnatal tamoxifen-induced *Dot1l*^{CondCART-KO} spontaneous osteoarthritis mouse model (*Dot1l*^{f/f} - *Acan-Cre-ER*^{+/−}). (B) X-ray images of the hind limbs of male *Dot1l*^{CondCART-KO} and control mice, 52 weeks after tamoxifen injection. (C) Three-dimensional reconstruction of a micro-computed tomography (μCT) image of the right knee of a male *Dot1l*^{CondCART-KO} and control mouse, 1 year after the tamoxifen injection (frontal view) and (D) hematoxylin-safraninO staining of the same knee (sagittal view). Scale bar: 500 μm. (B–D) Arrows point at ectopic bone formation. (E) Three-dimensional reconstructions of μCT images of the right knee of an individual *Dot1l*^{CondCART-KO} mouse at different timepoints after the tamoxifen injection (frontal view). The images are representative of six *Dot1l*^{CondCART-KO} mice and thirteen controls.

displayed more cartilage damage and osteophytosis than corresponding controls. The mutant mice also developed pronounced ectopic ossification over time. These findings demonstrate that DOT1L plays an important role in the prevention of ageing-related changes in the joint and reduces the risk for the development of spontaneous OA.

As traumatic joint injury strongly contributes to OA development in young adults²⁷, we studied the impact of *Dot1l*-deficiency after joint trauma. We performed DMM surgery on postnatal tamoxifen-induced *Dot1l*^{CondCART-KO} mice, as a post-traumatic OA model. *Dot1l*^{CondCART-KO} mice show more severe cartilage degradation, osteophyte formation and increased hypertrophy in the

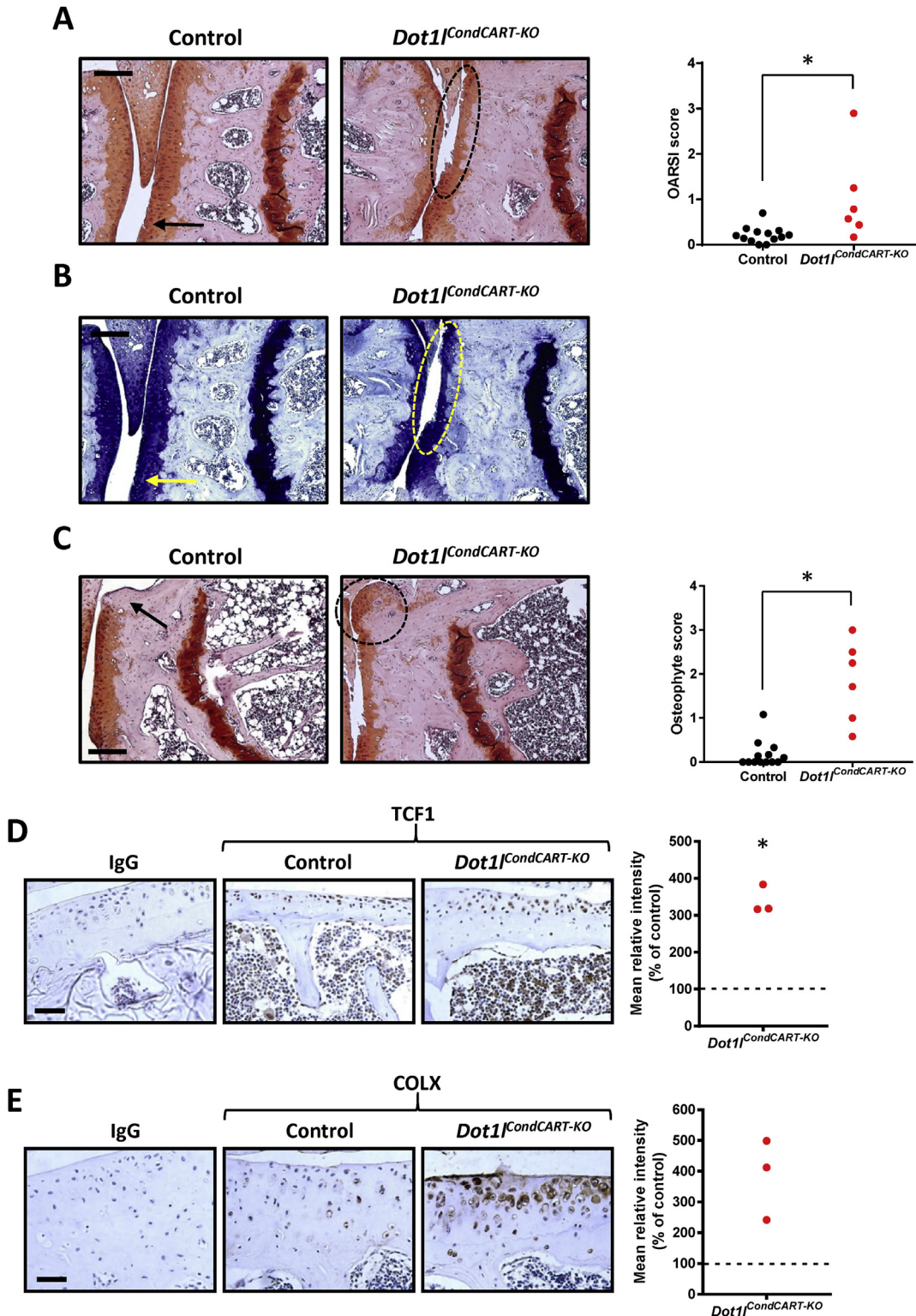


Fig. 7. Postnatal male *Dot1l^{CondCART-KO}* mice spontaneously develop osteoarthritis by the age of 14 months. (A) Frontal hematoxylin-safraninO staining of the medial quadrants and quantification of articular cartilage degradation at the medial tibia, evaluated by the OARSI scoring system, demonstrates more cartilage damage in male *Dot1l^{CondCART-KO}* mice, upon ageing. Data are presented as individual data points ($U = 9.5$, $*P = 0.007$ analysed by Mann–Whitney test). (B) Frontal toluidine blue staining of the medial quadrants. (A–B) The arrow points at a small cartilage lesion and the circle indicates a large cartilage lesion. (C) Frontal hematoxylin-safraninO stained sections of the medial tibia and quantification of the presence of osteophytes at the medial tibia, reveals more osteophytes in the aged male *Dot1l^{CondCART-KO}* mice knees compared to the control animals. Data are presented as individual data points ($U = 2$, $*P < 0.001$ analysed by Mann–Whitney test). The arrow points at a small osteophyte, the circle indicates a large osteophyte. (A–C) *Dot1l^{CondCART-KO}* mouse $n = 6$, control $n = 13$. Scale bar: 200 μ m. Immunohistochemical detection and quantification of TCF1 (discrepancy 239.4; $t(2) = 10.82$, $*P = 0.0084$, 95%CI of discrepancy = (144.2–334.7)) (D) and COLX (discrepancy 284; $t(2) = 3.762$, $P = 0.0639$, 95%CI of discrepancy = (−40.8–608.9)) (E) in the articular cartilage of the medial tibia of male *Dot1l^{CondCART-KO}* and control mice, aged for 14 months. (D–E) Data are presented as individual data points and the images are representative of three tamoxifen-induced *Dot1l^{CondCART-KO}* and three control mice. Scale bar: 50 μ m.

articular cartilage compared to control animals, after DMM surgery. Thus, these observations similarly demonstrate the importance of DOT1L to prevent OA development after joint trauma. To date, DOT1L is the only histone methyltransferase that has been reported to preserve cartilage homeostasis. Another histone methyltransferase, EZH2, was reported to have a key role in OA, but inhibition of its activity ameliorated disease development²⁸. Thus, DOT1L network is the only known epigenetic regulatory mechanism of histone modifications that prevents age-related and post-traumatic OA.

Both heterozygous *Dot1l*^{CART-KO} mice and tamoxifen-induced *Dot1l*^{CondCART-KO} mice displayed Wnt hyper-activation upon ageing and joint injury. Numerous independent studies suggest that Wnt signalling is one of the key pathways involved in OA^{13–16,29}. Both excessive activation and suppression of the Wnt cascade, in animal models, have been reported to result in OA^{15,29}. Thus, a tightly regulated Wnt pathway is crucial for joint homeostasis. Our data support that DOT1L achieves its protective role during ageing or upon joint trauma by preventing Wnt hyper-activation. We earlier reported that Wnt signalling hyper-activation is the major deleterious downstream effect of DOT1L inhibition in cartilage¹². Our novel data validate our mechanistic insights in translational OA mouse models. Notably, Zhu *et al.* reported that activation of Wnt signalling in articular chondrocytes in adult mice leads to the development of an OA-like phenotype with ectopic bone formation¹⁵. In our study, heterozygous *Dot1l*^{CART-KO} mice and tamoxifen-induced *Dot1l*^{CondCART-KO} mice spontaneously develop extensive ectopic bone formation in the hind limbs upon ageing, recapitulating characteristic features of the phenotype reported in conditional beta-catenin activation mice¹⁵.

The Wnt signalling pathway is also known to trigger chondrocyte hypertrophy in the articular cartilage. Increased hypertrophy was similarly observed in the articular cartilage of conditional beta-catenin activation mice¹⁵. Both *Dot1l*-deficient mouse strains similarly showed increased hypertrophy in articular cartilage, suggesting that epigenetic control of Wnt signalling by DOT1L is essential to prevent hypertrophic differentiation in the articular cartilage.

Interestingly, we observed that DOT1L activity is decreased in well-established non-transgenic OA mouse models, in particular, in the aged OA model and the DMM-induced OA model in wild-type mice. This observation parallels the decreased DOT1L activity in human OA cartilage compared to non-OA cartilage¹². These findings, both in mice and humans, point out that DOT1L's epigenetic control is lost during OA development. The specific factors that diminish DOT1L methylation in the articular cartilage during joint injury or ageing remain unknown and are an important area for further research. Targeting these factors may result in maintained DOT1L epigenetic control upon challenges in the joint environment.

Mouse models have limitations and so has our study. The joint biomechanics of mice are different from those of humans. This is important considering that mechanical stress in the joint is an essential factor in the development and progression of OA. Also, in contrast to humans, male mice develop more severe disease than females in OA mouse models and our experimental models were therefore limited to male mice^{30,31}. In addition, OA is a disease of the whole joint and thus mouse genetic approaches targeting specific cell types such as chondrocytes miss this complexity. These differences and limitations restrict the translation from mouse OA to human OA. Due to the complex breeding schemes and the long time required to age the animals, the number of mice in some of the experiments is rather low. The experiments were performed based on availability without a formal power calculation which limits the interpretation of the data. However, the consistent effect of DOT1L

loss of function in different models supports our overall observation. Our cartilage-specific approaches to target DOT1L also cannot exclude secondary differences in other tissues of the joint, linked with the severity of OA.

More insights into the DOT1L network and H3K79 methylation are also needed, to define the DOT1L network as a therapeutic target. Regulation of DOT1L activity is regarded as the primary mechanism to control H3K79 methylation and its downstream effects¹². As mentioned above, discovering the factors that regulate DOT1L activity, in particular, the factors that lead to loss of H3K79 methylation during joint trauma or upon ageing is of particular interest to develop DOT1L-based therapies for OA.

In OA, the articular cartilage is not uniform, macroscopically, there are areas with more cartilage damage and areas where the cartilage is better preserved within the same joint^{32–34}. Comparative analysis of articular chondrocytes also revealed that gene expression profiles differ between intact and damaged cartilage areas of the same joint³⁴. Thus, the articular chondrocytes are not a homogenous cell population in OA. Therefore, the individual health status of the cell may also determine the regulation of DOT1L activity and the H3K79 methylation maintenance.

In conclusion, this study demonstrates that *Dot1l* deficiency in mouse cartilage increases the susceptibility to develop spontaneous OA, and the severity of post-traumatic OA. This work establishes the essential role of DOT1L in the prevention of ageing-related osteoarthritic changes and the development of OA upon joint injury, through epigenetic negative control of Wnt signalling. Thus, targeting the DOT1L network to preserve its function upon joint trauma or in elderly patients may be of interest for the development of an effective therapy for OA.

Contributions

FMFC, RJL and SM were involved in study design, analysis of data and writing the manuscript. FMFC, AdR, LS and AH were involved in data acquisition. All authors were involved in interpretation of data and revising the article and approved final content of the article.

Conflict of interest

Leuven Research and Development, the technology transfer office of KU Leuven, has received consultancy and speakers fees on behalf of RJL from Galapagos and Samumed, active in the field of osteoarthritis. All other authors declare that they have no competing interests.

Funding

This work was supported by grants from Flanders Research Foundation (FWO-Vlaanderen), a C1 grant from KU Leuven and by the Excellence of Science Grant “Join-t-against-OA”. SM received a Marie-Curie Intra-European postdoctoral fellowship.

Data and materials availability

The data supporting the findings of this study are available within the article and from the corresponding author on reasonable request. B6.Cg-*Acantm1(cre/ERT2)Crm*/J mice were obtained from Dr. G. Bou-Gharios (currently University of Liverpool, UK) and the Kennedy Institute, Oxford, UK, under a Material Transfer Agreement.

References

1. Ramos YFM, Meulenbelt I. The role of epigenetics in osteoarthritis: current perspective. *Curr Opin Rheumatol* 2017;29:119–29.
2. Loeser RF. Aging processes and the development of osteoarthritis. *Curr Opin Rheumatol* 2013;25:108–13.

3. Goldring MB, Marcu KB. Epigenomic and microRNA-mediated regulation in cartilage development, homeostasis, and osteoarthritis. *Trends Mol Med* 2012;18:109–18.
4. Lotz M, Loeser RF. Effects of aging on articular cartilage homeostasis. *Bone* 2012;51:241–8.
5. Reynard LN. Analysis of genetics and DNA methylation in osteoarthritis: what have we learnt about the disease? *Semin Cell Dev Biol* 2017;62:57–66.
6. Simon TC, Jeffries MA. The epigenomic landscape in osteoarthritis. *Curr Rheumatol Rep* 2017;19: 30–30.
7. Feng Q, Wang H, Ng HH, Erdjument-Bromage H, Tempst P, Struhl K, et al. Methylation of H3-lysine79 is mediated by a new family of HMTases without a SET domain. *Curr Biol* 2002;12:1052–8.
8. Nguyen AT, Zhang Y. The diverse functions of Dot1 and H3K79 methylation. *Gene Dev* 2011;25:1345–58.
9. Steger DJ, Lefterova MI, Ying L, Stonestrom AJ, Schupp M, Zhuo D, et al. DOT1L/KMT4 recruitment and H3K79 methylation are ubiquitously coupled with gene transcription in mammalian cells. *Mol Cell Biol* 2008;28:2825–39.
10. Castaño-Betancourt MC, Cailotto F, Kerkhof HJ, Cornelis FMF, Doherty SA, Hart DJ, et al. Genome-wide association and functional studies identify the DOT1L gene to be involved in cartilage thickness and hip osteoarthritis. *Proc Natl Acad Sci USA* 2012;109:8218–23.
11. Castaño-Betancourt MC, Evans DS, Ramos YFM, Boer CG, Metrstry S, Liu Y, et al. Novel genetic variants for cartilage thickness and hip osteoarthritis. *PLoS Genet* 2016;12: e1006260.
12. Monteagudo S, Cornelis FMF, Aznar-Lopez C, Yibmantasiri P, Guns L-A, Carmeliet P, et al. DOT1L safeguards cartilage homeostasis and protects against osteoarthritis. *Nat Commun* 2017;8:15889.
13. Lories RJ, Corr M, Lane NE. To Wnt or not to Wnt: the bone and joint health dilemma. *Nat Rev Rheumatol* 2013;9:328–39.
14. Lories RJ, Peeters J, Bakker A, Tylzanowski P, Derese I, Schrooten J, et al. Articular cartilage and biomechanical properties of the long bones in *Frzb*-knockout mice. *Arthritis Rheum* 2007;56:4095–103.
15. Zhu M, Tang D, Wu Q, Hao S, Chen M, Xie C, et al. Activation of β -Catenin signaling in articular chondrocytes leads to osteoarthritis-like phenotype in adult β -Catenin conditional activation mice. *J Bone Miner Res* 2009;24:12–21.
16. Monteagudo S, Lories RJ. Cushioning the cartilage: a canonical Wnt restricting matter. *Nat Rev Rheumatol* 2017;13:670.
17. Testa G, Schaft J, van der Hoeven F, Glaser S, Anastassiadis K, Zhang Y, et al. A reliable lacZ expression reporter cassette for multipurpose, knockout-first alleles. *Genesis* 2004;38: 151–8.
18. Ovchinnikov DA, Deng JM, Ogunrinu G, Behringer RR. Col2a1-directed expression of Cre recombinase in differentiating chondrocytes in transgenic mice. *Genesis* 2000;26:145–6.
19. Cascio LL, Liu K, Nakamura H, Chu G, Lim NH, Chanalaris A, et al. Generation of a mouse line harboring a bi-transgene expressing luciferase and tamoxifen-activatable creERT2 recombinase in cartilage. *Genesis* 2014;52:110–9.
20. Glasson SS, Blanchet TJ, Morris EA. The surgical destabilization of the medial meniscus (DMM) model of osteoarthritis in the 129/SvEv mouse. *Osteoarthritis Cartilage* 2007;15:1061–9.
21. Glasson SS, Chambers MG, Van Den Berg WB, Little CB. The OARSI histopathology initiative – recommendations for histological assessments of osteoarthritis in the mouse. *Osteoarthritis Cartilage* 2010;18:S17–23.
22. Cornelis FMF, Monteagudo S, Guns L-AKA, den Hollander W, Nelissen RGHH, Storms L, et al. ANP32A regulates ATM expression and prevents oxidative stress in cartilage, brain, and bone. *Sci Transl Med* 2018;10.
23. Stoop R, Van Der Kraan Peter M, Buma P, Hollander AP, Billinghurst RC, Poole AR, et al. Type II collagen degradation in spontaneous osteoarthritis in C57BL/6 and BALB/c mice. *Arthritis Rheum* 1999;42:2381–9.
24. Pitsillides AA, Beier F. Cartilage biology in osteoarthritis – lessons from developmental biology. *Nat Rev Rheumatol* 2011;7: 654.
25. van der Kraan PM, van den Berg WB. Chondrocyte hypertrophy and osteoarthritis: role in initiation and progression of cartilage degeneration? *Osteoarthritis Cartilage* 2012;20: 223–32.
26. Loeser RF. Aging and osteoarthritis. *Curr Opin Rheumatol* 2011;23:492–6.
27. Stiebel M, Miller LE, Block JE. Post-traumatic knee osteoarthritis in the young patient: therapeutic dilemmas and emerging technologies. *Open Access J Sports Med* 2014;5: 73–9.
28. Chen L, Wu Y, Wu Y, Wang Y, Sun L, Li F. The inhibition of EZH2 ameliorates osteoarthritis development through the Wnt/ β -catenin pathway. *Sci Rep* 2016;6:29176.
29. Zhu M, Chen M, Zuscik M, Wu Q, Wang Y-J, Rosier RN, et al. Inhibition of β -Catenin signaling in articular chondrocytes results in articular cartilage destruction. *Arthritis Rheum* 2008;58:2053–64.
30. Ma HL, Blanchet TJ, Peluso D, Hopkins B, Morris EA, Glasson SS. Osteoarthritis severity is sex dependent in a surgical mouse model. *Osteoarthritis Cartilage* 2007;15:695–700.
31. Silberberg M, Silberberg R. Role of sex hormone in the pathogenesis of osteoarthritis of mice. *Lab Invest* 1963;12:285–9.
32. Fukui N, Ikeda Y, Ohnuki T, Tanaka N, Hikita A, Mitomi H, et al. Regional differences in chondrocyte metabolism in osteoarthritis: a detailed analysis by laser capture microdissection. *Arthritis Rheum* 2008;58:154–63.
33. Geyer M, Grässle S, Straub RH, Schett G, Dinser R, Grifka J, et al. Differential transcriptome analysis of intraarticular lesional vs intact cartilage reveals new candidate genes in osteoarthritis pathophysiology. *Osteoarthritis Cartilage* 2009;17:328–35.
34. Sato T, Konomi K, Yamasaki S, Aratani S, Tsuchimochi K, Yokouchi M, et al. Comparative analysis of gene expression profiles in intact and damaged regions of human osteoarthritic cartilage. *Arthritis Rheum* 2006;54:808–17.